as the study of structure–function relationships.

ACKNOWLEDGMENTS

We thank Dr. Y. Yakir and Bio-Yeda Ltd. (now Bio-Makor Ltd.) for their participation in the initial stages of purification of THF and Y. Hacham, I. Lehavot, S. Tel-Or, M. David, S. Lourie, and A. Levi for dedicated technical help.

Registry No. THF, 63340-72-7; THF-γ2, 107489-37-2.

REFERENCES

Bach, J.-F., & Carnaud, C. (1976) *Prog. Allergy 21*, 342–408.
Bach, J.-F., Dardenne, M., & Pleau, J.-M. (1977) *Nature (London) 266*, 55–57.
Gillis, S. E., & Watson, J. (1981) *Immunol. Rev. 54*, 81–109.
Hand, T. L., Ceglowski, D., Damrongsak, D., & Friedman, H. (1970) *J. Immunol. 105*, 442–450.
Handzel, Z. T., Bentwich, Z., Burstein, R., Segal, O., Berner, Y., Levin, S., Pecht, M., Netzer, L., Trainin, N., Buchner, V., & Burstein, Y. (1985) *Clin. Immunol. Newslett. 6*, 68–71.
Handzel, Z. T., Berner, Y., Segal, O., Burstein, Y., Buchner, V., Pecht, M., Levin, S., Burstein, R., Milchan, R., Bentwich, Z., Ben-Ishai, Z., & Trainin, N. (1987) *Int. J. Immunopharmacol. 9*, 165–173.
Hunkapiller, M. W., & Hood, L. E. (1983) *Methods Enzymol. 91*, 486–493.
Kook, A., & Trainin, N. (1974) *J. Exp. Med. 139*, 193–207.
Kook, A. I., Yakir, Y., & Trainin, N. (1975) *Cell. Immunol. 19*, 151–157.
Levey, R. H., Trainin, N., Law, L. W., Black, P. H., & Rowe, W. P. (1963a) *Science (Washington, D.C.) 142*, 483–485.
Levey, R. H., Trainin, N., & Law, L. W. (1963b) *J. Natl. Cancer. Inst. (U.S.) 31*, 199–217.
Merrifield, R. B. (1963) *J. Am. Chem. Soc. 85*, 2149–2154.
Osoba, D., & Miller, J. F. A. P. (1963) *Nature (London) 199*, 653–654.
Rotter, V., & Trainin, N. (1975) *Cell. Immunol. 16*, 413–421.
Small, M., & Trainin, N. (1967) *Nature (London) 216*, 377–379.
Trainin, N., & Linker-Israeli, M. (1967) *Cancer Res. 27*, 309–313.
Trainin, N., Small, M., Zippori, D., Umiel, T., Kook, A. I., & Rotter, V. (1975) in *The Biological Activity of Thymic Hormones* (Bekkum, D. W., Ed.) pp 117–144, Kooker Scientific, Rotterdam.
Trainin, N., Handzel, Z. T., & Pecht, M. (1985) *Thymus 7*, 137–150.
Trainin, N., Burstein, Y., Buchner, V., Pecht, M., Netzer, L., Bentwich, Z., Burstein, R., Berner, Y., Segal, O., & Handzel, Z. T. (1986) in *Viruses, Immunity & Immunodeficiency* (Szentivanyi, A., & Friedman, H., Eds.) pp 313–319, Plenum, New York.
Umiel, T., & Trainin, N. (1975) *Eur. J. Immunol. 5*, 85–88.
Zatz, M. M., Oliver, J., Sztein, M. B., Skotnicki, A. B., & Goldstein, A. L. (1985) *J. Biol. Response Modif. 4*, 365–376.

Peptides Mimicking the Flap of Human Renin: Synthesis, Conformation, and Antibody Recognition†

Jean-Alain Fehrentz,* Annie Heitz, René Seyer, Pierre Fulcrand, René Devilliers, and Bertrand Castro
Centre CNRS-INSERM de Pharmacologie-Endocrinologie, rue de la Cardonille, 34094 Montpellier Cedex, France

Frédéric Heitz
Laboratoire de Physico-chimie des Systèmes Polyphasés, 34033 Montpellier, France

Claude Carelli
Inserm U 36, 17, rue du Fer à Moulin, 75005 Paris, France

Received May 28, 1987; Revised Manuscript Received October 7, 1987

ABSTRACT: Four peptides related to human renin flap region have been synthesized. Two of them are ring closed through appropriately designed disulfide bridges. Structure analysis involving IR and NMR techniques and recognition by polyclonal human renin antibodies provides support for a β-hairpin secondary structure of the cyclized peptides identical with that presented by the flap section in the speculative human renin model [Blundell, T., Sibanda, B. L., & Pearl, L. (1983) *Nature (London) 304*, 273–275; Sibanda, B. L., Blundell, T., Hobart, P. M., Fogliano, M., Bindra, J. S., Dominy, B. W., & Chirgwin, J. M. (1984) *FEBS Lett. 174*, 102–111].

Renin (EC 3.4.23.15), an aspartyl protease, plays a key role in the regulation of blood pressure homeostasis. It cleaves its substrate angiotensinogen to release angiotensin I which is then converted into angiotensin II, a potent vasoconstrictor octapeptide, by the action of a carboxydipeptidase. Apart from its primary structure which has been recently established from the sequence of its cDNA (Imai et al., 1983), no experimental data have been obtained concerning the structure of renins. Several renin three-dimensional models have been proposed (Blundell et al., 1983; Sibanda et al., 1984; Akahane et al., 1985; Carlson et al., 1985) on the basis of X-ray diffraction data which show that, except for small deviations, there is a striking similarity with the structures of pepsins (Tang et al., 1978). These models can be used as a working hypothesis in order to predict, at least in part, the conformation of renins.

The aspartyl proteases are characterized by a major groove between the C- and N-terminal domains and in addition by

† This work was supported by INSERM and CNRS.
* Correspondence should be addressed to this author.

0006-2960/88/0427-4071$01.50/0

Table I: Physical Characteristics of the Peptides

	sequence	peptide identification	HPLC capacity factor, k'	amino acid analysis
peptide I	LRYSTGTVSG	[81–90]human renin	2.7 (15% CH_3CN)	Leu, 0.99 (1); Arg, 1.02 (1); Tyr, 0.95 (1); Ser, 2.05 (2); Thr, 1.99 (2); Gly, 2.03 (2); Val, 1.01 (1)
peptide II	TELTLRYSTGTVSGFLS	[77–93]human renin	5.1 (27% CH_3CN)	Thr, 4.05 (4); Glu, 0.98 (1); Leu, 3.03 (3); Arg, 1.01 (1); Tyr, 0.97 (1); Ser, 3.08 (3); Gly, 2.02 (2); Val, 1.02 (1); Phe, 0.95 (1)
peptide III	CLRYSTGTVC	(Cys^{80},Cys^{89})-[80–89]human renin	3.3 (17% CH_3CN)	Leu, 1.01 (1); Arg, 0.98 (1); Tyr, 0.95 (1); Ser, 1.08 (1); Thr, 1.95 (2); Gly, 0.97 (1); Val, 0.95 (1)
peptide IV	CLTLRYSTGTVSGC	(Cys^{78},Cys^{91})-[78–91]human renin	9.1 (18% CH_3CN)	Leu, 1.98 (2); Thr, 3.05 (3); Arg, 0.97 (1); Tyr, 0.98 (1); Ser, 2.05 (2); Gly, 2.02 (2); Val, 1.01 (1)

```
70        75        80        85
K W S I S Y G A G A S A S G N A V.....Endothiapepsin

T W S I S Y G D G S S A S G N V F.....Penicillopepsin

T W S I S Y G D G S S A S G I L A.....Rhizopuspepsin

D F T I H Y G S G R V  K G F L S.....Mouse Submaxillary renin

E L T L R Y S T G T V  S G F L S.....Human renin
```

FIGURE 1: Alignment of several aspartyl protease sequences in the flap region. The amino acids are expressed in the single-letter code. The numbering is based on the sequence of porcine pepsin. The sequence of endothia pepsin is not a chemical sequence but is derived from X-ray analysis.

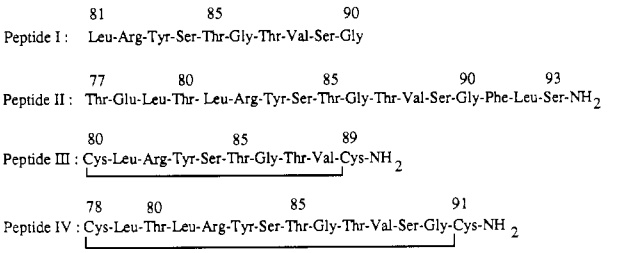

FIGURE 2: Sequences of the synthesized peptides. The numbering is based on the sequence of human renin.

the existence of an extended β-hairpin loop forming a flexible region termed the "flap" which protrudes. Its mobility, which has been demonstrated experimentally (James & Sielecki, 1985, 1986), suggests that the flap could play a major role in the biological activity of the aspartyl proteases. In Figure 1, the flap sequences of several aspartyl proteases are compared and indicate that a residue deletion occurs on going from the pepsins to the renins. This figure also shows that glycine-76 (porcine pepsin numbering), which is invariant in all aspartyl proteases, is replaced in human renin by a serine. In order to determinate the influence of these two modifications, it was of great interest to know the secondary structure of the human renin flap.

In this paper it is shown that peptides with the same sequence as the flap section of human renin can adopt a large β-hairpin structure when forced by ring closures through disulfide bridges between two cysteyl residues correctly placed. This β-hairpin structure is ascertained by ^1H NMR and IR studies and is selectively recognized by polyclonal antibodies raised against human renin.

Materials and Methods

Choice of the Peptides. As mentioned above, the main difference on going from the pepsins to the renins lies in the deletion of one residue. In order to maintain the overall feature of the flap β-hairpin, this deletion can cause either a modification of the side-chain orientation of one strand of the hairpin or a modification of the reversal type of the peptide chain, going from a β to a γ turn or vice versa. Discrimination between these possibilities can easily be achieved through ^1H NMR spectrometry. Indeed, $C_\alpha H$–$C_\alpha H$ NOEs[1] between facing residues are expected, thus allowing the localization of the reversal. In this study we considered first two linear peptides, a 10-residue [81–90]human renin (I) and a 17-residue [77–93]human renin (II). Then on the basis of the results obtained mainly on II, in order to improve the stability of the expected structure two homologous cyclic peptides, (Cys^{80},Cys^{89})-[80–89]human renin (III) and (Cys^{78},Cys^{91})-[78–91]human renin (IV) were designed especially for both the conformation study and the biological activity. The sequences of the four synthesized peptides are given in Figure 2.

Peptide Synthesis. Table I lists the characteristics of the peptides prepared for this study. The peptides were synthesized by the solid-phase technique with either chloromethylated resin for I or *p*-methylbenzhydrylamine resin for II, III, and IV. The side chain protecting groups were the following: *O*-(2,6-dichlorobenzyl) (tyrosine), *O*-benzyl (glutamic acid, serine, threonine), *N*-tosyl (arginine), and *S*-(*p*-methoxybenzyl) (cysteine). The temporary protection of the N^α function was *tert*-butyloxycarbonyl, which was removed in 30 min with a trifluoroacetic acid/dichloromethane/ethanedithiol solution (30/70/5). The coupling reactions were carried out with a twofold excess of protected amino acid and (benzotriazol-1-yloxy)tris(dimethylamino)phosphonium hexafluorophosphate (BOP) (Dormoy & Castro, 1979; Le Nguyen & Rivier, 1986). The protected peptidyl resin was treated with anhydrous hydrogen fluoride containing 10% anisole for 1 h at 0 °C. After removal of the hydrogen fluoride, the residue was washed with diethyl ether and extracted with water or 1 M acetic acid, and the aqueous solution was lyophilized. Peptides I, II, and III were purified by reverse-phase high-performance liquid chromatography while IV was first cyclized and then purified as the others.

Cyclization of III and IV. The air cyclization process was followed by Ellman's test and by HPLC analysis with a dual-wavelength apparatus monitoring at 214 and 254 nm, the absorbance ratios at these wavelengths between the cyclized peptide and the linear one being different (Figure 3). Peptide III was purified by HPLC before cyclization. The disulfide bond formation was completed in 1 h by air oxidation of an aqueous solution (pH 8) at a concentration of 0.3 mg of peptide/mL. The oxidized product was then recovered by lyophilization and purified once more. The oxidation of IV (Figure 3) was performed on the crude peptide under the same

[1] Abbreviations: ELISA, enzyme-linked immunosorbent assay; PBS, phosphate-buffered saline; BSA, bovine serum albumin; Tris, tris(hydroxymethyl)aminomethane; HPLC, high-performance liquid chromatography; NOE, nuclear Overhauser effect; DMSO, dimethyl sulfoxide.

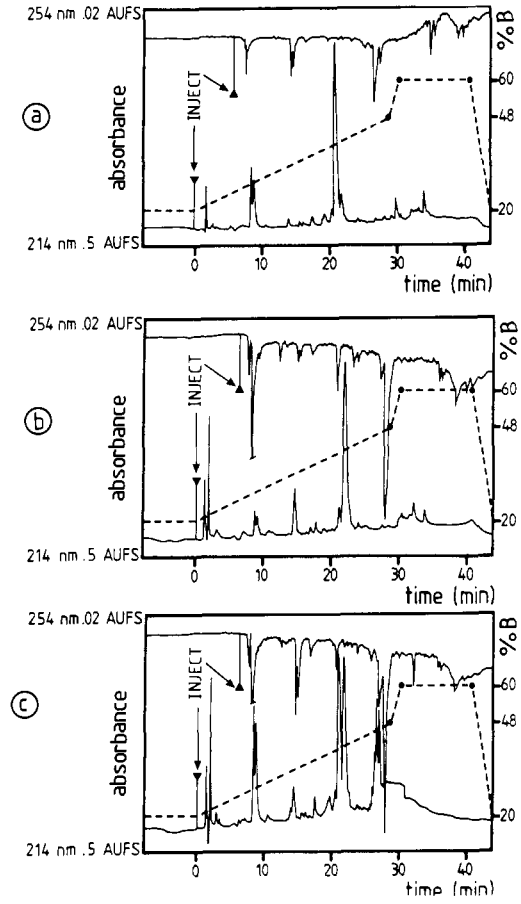

FIGURE 3: Reverse-phase HPLC of peptide IV: (a) crude product after HF cleavage, (b) crude mixture after 45-min oxidation process, and (c) mixture of unoxidized and oxidized crude product. The oxidation monitoring was done on a C18 column (4 × 250 mm, 5-μm granulometry, Lichrosorb Merck). Solvent A is 0.1% trifluoroacetic acid in water, and solvent B is 0.1% trifluoroacetic acid in 60% acetonitrile. The column was run at ambient temperature with a flow rate of 1 mL/min and a linear gradient of 1% solvent B/min. Absorbance was measured at 214 (bottom) and 254 nm (top).

conditions as peptide III, and it was purified after cyclization.

Peptide Purity. The peptide homogeneity was controlled by HPLC in isocratic and gradient elution mode at 214 and 254 nm; their capacity factor (k') is given in Table I as is also their amino acid analysis. Purity of the peptides was assessed by amino acid analysis using automated precolumn derivatization with *o*-phthalaldehyde with a Waters system. Capacity factor was calculated in the following conditions: column, C18 reversed-phase Lichrosorb Merck (4 × 250 mm, 5 μm); monitoring at 214 and 254 nm with an isocratic eluent system (acetonitrile/water) containing 0.1% trifluoroacetic acid; flow rate, 1.5 mL/min.

Binding of Peptides to Renin Antibodies. The binding of the peptides to renin antibodies was tested by ELISA with 11 renin antisera (R11, R12, R14, R15, R21, R22, R24, R25, R26, Donc, and Bof) raised in rabbits after immunization against pure human active renin obtained from a juxtaglomerular cell tumor as previously described (Galen et al., 1984). This tumoral renin was found to have the same biochemical, biophysical, and immunological characteristics as human renal renin (Galen et al., 1979).

For ELISA, plastic microtiter plates (Falcon 3915 Pro-bind, Becton Dickinson Labware, CA) were coated with 50 μL of peptide solution at 5 μg/mL of Tris-HCl buffer, 0.1 M (pH 9.6). After 90 min at 37 °C, the plates were washed 3 times with Tween containing phosphate-buffer saline (PBS, 0.1% Tween, pH 7.4). After saturation of the nonspecific binding sites with 1% bovine serum albumin (BSA, radioimmunoassay grade, obtained from Sigma) in 0.1 M PBS, pH 7.4, 50 μL of a 1:500 dilution in PBS–1% BSA, pH 7.4, of polyclonal antibodies in PBS was added in peptide-coated duplicate wells and incubated for 1 h at 37 °C. The plates were washed 3 times with PBS–0.1% Tween, and 50 μL of alkaline phosphatase labeled sheep anti-rabbit IgG was added and incubated 1 h at 37 °C. Additional extensive washing with PBS–0.1% Tween was followed by incubation with 150 μL of alkaline phosphatase substrate (two tablets of Sigma 104-105/10 mL) dissolved in 0.1 M glycine–NaOH buffer, pH 10.4, containing 1 M $MgCl_2$ and $ZnCl_2$. The enzymatic reaction was allowed to proceed for 2 h at 37 °C and stopped by addition of 50 μL of 1.5 M Na_2CO_3. Absorbance was read at 405 nm in a Titerteck Multiskan ELISA reader (Flow Laboratories). Titer was expressed as the ratio between absorbance of the specific renin antibody (A) and the absorbance of the negative control (A_0) consisting of pooled normal rabbit sera at the same dilution. Only ratio values greater than 2 were interpreted as significant.

Instrumentation: IR and NMR Spectroscopy. Infrared spectra were recorded on a 983 Model Perkin-Elmer spectrograph. Samples for NMR spectrometry were prepared at 12–20 mM peptide concentration in DMSO-d_6 and spectra were obtained at 32 °C. ^{1}H NMR spectra were collected on a Bruker 360-MHz spectrometer equipped with an Aspect 2000 computer and operated in the Fourier transform mode with quadrature detection. One-dimensional spectra were recorded with a 4-kHz sweep and 16K or 32K data words were employed. Proton resonance assignments were obtained by COSY (Aue et al., 1976; Nagayama et al., 1980), RELAY (Wagner, 1983), and NOESY (Bodenhausen et al., 1984; Otting et al., 1986) spectra. For the RELAY experiments, total delays of 60 ms during the mixing period were used. Mixing times of 150–300 ms were used for NOESY spectra. The COSY and RELAY (magnitude) spectra were obtained with 2048 points for each values of t_1. There were 512 t_1 measurements of 64 transients each leading to a digital resolution of 3.2 Hz/point. The NOESY (phase-sensitive mode) were obtained with 4096 points for each value of t_1. There were 256 t_1 measurements of 256 transients each leading to a digital resolution of 1.6 Hz/point in ω_2 and 12.5 Hz/point in ω_1. Before Fourier transform the time domain matrix was multiplied in both dimensions by a sine bell function without phase shift for COSY and by a $\pi/8$ phase shifted in t_2 and a $\pi/4$ phase shifted in t_1 for NOESY.

Conformational Investigations in DMSO

Infrared Spectroscopy. When dissolved in DMSO, all four peptides have infrared spectra which show strong similarities as they are characterized by the presence of two amide I bands (C=O stretching). They lie on one hand at 1692 cm^{-1} and on the other at 1670 cm^{-1} (shoulder) for I, 1664 cm^{-1} for II, and 1652 cm^{-1} for III and IV. These spectra favor the existence of, at least, two types of carbonyl groups and are in accordance with a conformation based on two strands linked through hydrogen bonds as expected for a hairpin structure. Owing to its high wavenumber position, the 1692-cm^{-1} band can be attributed to the nonbonded carbonyls while the others correspond to hydrogen-bonded carbonyl groups. Furthermore, the respective positions of these latters reveal that the interstrand hydrogen bonds are strengthened on going from the linear to the cyclic peptides, thus indicating that the latters have a lower backbone flexibility.

^{1}H NMR Studies. The NMR characteristics of the four peptides are reported in Tables II and III. Figure 4 shows

Table II: ^{1}H NMR Data on Peptide NH Resonances: Chemical Shifts[a] (ppm), $^3J_{NH-C_\alpha H}$ (Hz), and Temperature Coefficients (ppm/deg × 10^3)

residue	peptide I	peptide II	peptide III	peptide IV
Glu- or Cys-78				
NH		8.61		
$^3J_{NH-C_\alpha H}$		7.6		
$\Delta\delta/\Delta T \times 10^3$		−3.3		
Leu-79				
NH		8.18		8.67
$^3J_{NH-C_\alpha H}$		7.6		8.2
$\Delta\delta/\Delta T \times 10^3$		−3.3		−2.0
Thr- or Cys-80				
NH		7.87		8.31
$^3J_{NH-C_\alpha H}$		8.6		8.6
$\Delta\delta/\Delta T \times 10^3$		−4.6		−9.2
Leu-81				
NH		7.77	8.76	8.19
$^3J_{NH-C_\alpha H}$		8.6	8.8	8.7
$\Delta\delta/\Delta T \times 10^3$		−2.7	−2.3	−6.2
Arg-82				
NH	8.55	7.94	8.62	8.36
$^3J_{NH-C_\alpha H}$	8.1	8.3	8.3	9.0
$\Delta\delta/\Delta T \times 10^3$	−2.3	−2.9	−4.6	−6.3
Tyr-83				
NH	8.04	7.84	8.05	7.97
$^3J_{NH-C_\alpha H}$	8.3	8.6	9.3	9.0
$\Delta\delta/\Delta T \times 10^3$	−3.3	−3.0	−2.3	−3.0
Ser-84				
NH	8.21	8.16	9.05	8.73
$^3J_{NH-C_\alpha H}$	7.5	8.3	3.7	5.8
$\Delta\delta/\Delta T \times 10^3$	−5.1	−5.0	−9.5	−11.8
Thr-85				
NH	7.76	7.77	7.01	7.24
$^3J_{NH-C_\alpha H}$	7.6	8.6	9.0	8.3
$\Delta\delta/\Delta T \times 10^3$	−2.6	−2.7	+3.0	+3.9
Gly-86				
NH	8.04	8.04	7.34	7.60
$^3J_{NH-C_\alpha H}$	Σ11.1	Σ11	7.6–2.5	6.4–3.2
$\Delta\delta/\Delta T \times 10^3$	−2.3	−2.3	0	+3.7
Thr-87				
NH	7.81	7.81	8.37	8.05
$^3J_{NH-C_\alpha H}$	8.4	8.6	8.5	8.6
$\Delta\delta/\Delta T \times 10^3$	−3.3	−3.2	−6.5	−7.5
Val-88				
NH	7.74	7.78	8.37	8.11
$^3J_{NH-C_\alpha H}$	8.2	7.6	9.3	9.4
$\Delta\delta/\Delta T \times 10^3$	−2.6	−2.7	−5.2	−6.1
Ser- or Cys-89				
NH	7.94	7.96	8.91	8.41
$^3J_{NH-C_\alpha H}$	7.8	7.9	9.3	7.5
$\Delta\delta/\Delta T \times 10^3$	−4.0	−3.8	−5.9	−8.2
Gly-90				
NH	8.02	7.99		8.47
$^3J_{NH-C_\alpha H}$	Σ11.8	Σ11		Σ11
$\Delta\delta/\Delta T \times 10^3$	−4.5	−3.2		−7.6
Phe- or Cys-91				
NH		8.04		8.19
$^3J_{NH-C_\alpha H}$		7.9		8.7
$\Delta\delta/\Delta T \times 10^3$		−3.4		−3.1
Leu-92				
NH		8.18		
$^3J_{NH-C_\alpha H}$		7.6		
$\Delta\delta/\Delta T \times 10^3$		−4.6		
Ser-93				
NH		7.67		
$^3J_{NH-C_\alpha H}$		7.6		
$\Delta\delta/\Delta T \times 10^3$		−3.4		

[a] Chemical shifts relative to DMSO resonance (2.5 ppm): 32 °C; concentration, 12–20 mM.

the NH spectral region of peptide II.

(*A*) *Resonance Assignments.* Identification of the amino acids systems was accomplished by means of COSY spectra. RELAY spectra were acquired when the assignment of a particular amide proton to a specific spin system was not possible owing to severe overlapping in the $C_\alpha H$ region.

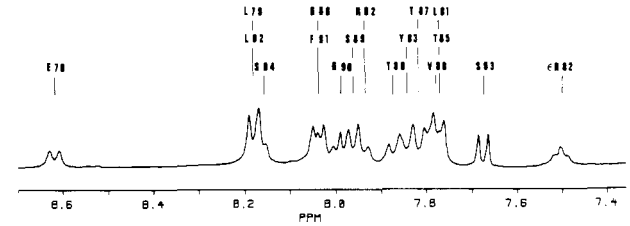

FIGURE 4: One-dimensional 360-MHz NH region spectrum of peptide II in DMSO.

Table III: Chemical Shifts[a] (ppm) of Protons Other Than NH of the Four Peptides

residue	peptide I	peptide II	peptide III	peptide IV
Thr-77				
α		3.59		
β		3.78		
γ		1.14		
Glu- or Cys-78				
α		4.37		4.15
β		1.88–1.76		3.09–2.99
γ		2.31–2.24		
Leu-79				
α		4.39		4.56
β		1.45		1.47
γ		1.60		1.64
δ		0.89–0.84		0.89
Thr- or Cys-80				
α		4.22	4.51	4.45
β		3.96	3.07–2.81	3.83
γ		1.02		0.98
Leu-81				
α	3.80	4.30	4.51	4.48
β	1.48	1.43	1.53	1.50
γ	1.58	1.60	1.60	1.47
δ	0.87–0.86	0.87–0.84	0.90–0.85	0.85–0.81
Arg-82				
α	4.35	4.23	4.42	4.35
β	1.66–1.51	1.64–1.45	1.62–1.40	1.59–1.40
γ	1.49	1.45	1.40	1.40
δ	3.09	3.05	3.03	3.04
ε	7.64	7.50	7.35	7.39
Tyr-83				
α	4.52	4.50	4.61	4.56
β	2.95–2.70	2.93–2.69	3.11–2.88	3.03–2.78
Ser-84				
α	4.42	4.40	4.01	4.11
β	3.65–3.58	3.64–3.56	3.74	3.68
Thr-85				
α	4.23	4.21	4.03	4.09
β	4.07	4.07	4.28	4.22
γ	1.07	1.07	1.04	1.02
Gly-86				
α	3.85–3.79	3.85–3.78	4.33–3.64	4.15–3.71
Thr-87				
α	4.34	4.33	4.84	4.71
β	3.97	3.96	3.80	3.89
γ	1.03	1.02	1.01	0.99
Val-88				
α	4.24	4.23	4.45	4.42
β	2.03	2.01	1.98	1.98
γ	0.84	0.84–0.81	0.91–0.88	0.85–0.83
Ser- or Cys-89				
α	4.33	4.27	4.61	4.67
β	3.58–3.55	3.59–3.52	3.14–2.86	3.61–3.57
Gly-90				
α	3.76	3.69–3.61		3.89
Phe- or Cys-91				
α		4.53		4.44
β		3.05–2.74		3.34–2.86
Leu-92				
α		4.30		
β		1.51		
γ		1.60		
δ		0.86–0.82		

[a] Chemical shifts relative to DMSO resonance (2.5 ppm): 32 °C; concentration, 12–20 mM.

Table IV: Characteristic Observed NOEs in the Turn and between the Two Strands of the Hairpin[a]

	peptide II	peptide III	peptide IV
turn	NH Thr-85–NH Gly-86	NH Ser-84–NH Thr-85	NH Ser-84–NH Thr-85
		NH Thr-85–NH Gly-86	NH Thr-85–NH Gly-86
		NH Thr-85–Hα Ser-84	NH Thr-85–Hα Ser-84
		NH Gly-86–Hβ Thr-85	NH Gly-86–Hβ Thr-85
interstrand	Hα Arg-82–Hα Thr-87	Hα Arg-82–Hα Thr-87	Hα Thr-80–Hα Ser-89
		Hα Cys-80–Hα Cys-89	Hα Arg-82–Hα Thr-87
			Hα Cys-78–Hα Cys-91
		NH Leu-81–NH Val-88	NH Leu-79–Hα Cys-91
		NH Leu-81–Hα Cys-89	NH Leu-81–Hα Ser-89
		NH Tyr-83–NH Gly-86	NH Tyr-83–Hα Thr-87
		NH Tyr-83–Hα Thr-87	NH Val-88–Hα Arg-82
		NH Val-88–Hα Arg-82	NH Gly-90–Hα Thr-80

[a] Note that in II, NOE between Thr-80 $C_\alpha H$ and Ser-89 $C_\alpha H$ could not be detected, if any, due to the superposition of the corresponding signals (see Table III).

(*B*) *Sequential Resonance Assignments.* The connectivities between $C_\alpha H_i$ and NH_{i+1} protons were established from NOESY spectra (Wuthrich, 1983). The combined COSY–NOESY contour map obtained for peptide IV (Figure 5) shows the NOE connectivities between the N*H*'s and the C_α protons of their respective preceding residues while the COSY portion shows the J_{NH-CH} connectivities within the same residue.

(*C*) *Conformational Elements.* The $^3J_{NH-C_\alpha H}$ coupling constants, which are listed in Table II, lie in the 8.5–9.5-Hz range for several successive residues. For example, in peptide IV, these residues correspond to sequences 79–83 and 87–91. These large coupling constants suggest that the corresponding residues are engaged in an extended conformational state (Kishore & Balaram, 1984; Pardi et al., 1984). This conclusion is corroborated by one-dimensional NOE experiments which reveal that the interresidue NH_{i+1}–$C_\alpha H_i$ NOEs are stronger than the intraresidue ones: 12 and 4%, respectively (Billeter et al., 1982; Kuo & Gibbons, 1980).

Figure 6b shows the NOESY spectrum of peptide IV in the $C_\alpha H$ region in which the cross-peaks arising from short $C_\alpha H$–$C_\alpha H$ distances are indicated. This spectrum clearly reveals that the $C_\alpha H$'s of residues 78, 80, and 82 are in the vicinity of those of residues 91, 89, and 87, respectively. These NOEs (Wuthrich et al., 1984; Wagner et al., 1981) together with other interresidue N*H*–$C_\alpha H$ and N*H*–N*H* NOEs which are summarized in Table IV and shown for peptide III in the N*H* region in Figure 6a, are typical of those expected for two antiparallel strands forming a β sheet (Figure 7). It must be noticed that all the expected interstrand NOEs are observed for peptide III and IV (Table IV and Figure 8). All the above data lead us to propose that the structure of III and IV is based on an antiparallel β sheet involving sequences 80–82 and 87–89 for peptide III and sequences 78–82 and 87–91 for peptide IV. As a sheet structure is stabilized by interstrand hydrogen bonds with an antiparallel orientation of the successive NH bonds, each strand is characterized by an alternation of bonded and nonbonded NH's. Therefore, temperature-induced variations of the chemical shifts of the various NH's should reveal an alternation of low and high temperature coefficients, respectively. Experimentally, residues 81 and 83 in peptide III and residues 79 and 83 in peptide IV have low temperature coefficients (Figure 9 and Table II), but the situation is less clear for the other residues such as 88 in peptide III or 81, 88, and 90 in peptide IV. Taking into account the interstrand NOEs which indicate that these NH's point toward the "interior" of the sheet, we conclude that they are engaged in weaker hydrogen bonds than the other hydrogen-bonded NH's. This latter conclusion is confirmed by a solvent titration in DMSO–chloroform mixtures (the four peptides are insoluble in pure chloroform). Examination of Table V in which the dependence of the chemical shifts of the NH's of III are gathered reveals that when the amount of chloroform is decreased, the N*H*'s which are expected to be nonbonded show a strong downfield shift while the others do not or slightly move upfield. That Val-88 N*H* has an intermediate behavior suggests that it is engaged in an hydrogen bond but in a weaker manner than those of the other residues such as Leu-81 or Tyr-83.

The existence of an antiparallel β sheet implies the presence of a chain reversal located in the 83–86 sequence. Several arguments suggest that the reversal is made of a β turn. Indeed, (i) it contains four residues, (ii) the NH of Gly-86, which shows a positive or close to zero $\Delta\delta/\Delta T$, points toward the interior of the sheet, and (iii) the $^3J_{NH-C_\alpha H}$ coupling constant of residue 84 is small as expected for a residue in position $i + 1$ of a β turn. Furthermore, according to Chou and Fasman (1978), a sequence with Ser-84 and Gly-86 which correspond to positions $i + 1$ and $i + 3$ of the turn is a very favorable situation for a β turn. Certain data such as the strong Ser-84 $C_\alpha H$–Thr-85 N*H* NOE suggest that it could be of the II type. However, the temperature coefficient of the Thr-85 N*H* (residue $i + 3$ of the turn) (see Table II) suggests that this group could also participate in an hydrogen bond while it is expected to be free in a classical β turn. Such a situation is reminiscent of that observed by Gierasch et al. (1981) for *cyclo*-(Gly-Pro-Gly)$_2$. These authors proposed a particular type of β turn in which the carbonyl group of residue i is engaged with two N*H*'s, those of residues $i + 2$ and $i + 3$. For the peptides considered here, this corresponds to the Tyr-83 carbonyl (residue i) which is involved in two hydrogen bonds with the N*H*'s of Thr-85 (residue $i + 2$) and Gly-86 (residue $i + 3$). The finding of a strong Thr-85 N*H*–Gly-86 N*H* NOE favors this particular feature of the β turn. In addition, from the temperature coefficients of the O*H*'s of residues Ser-84, Thr-85, and Thr-87 ($\Delta\delta/\Delta T \times 10^3$ = 9.8, 3.4, and 5.1, respectively), it appears that for peptide IV the O*H* of the Thr-85 residue could also participate in a hydrogen bond. Examination of molecular models leads to the proposal of a Ser-84 CO–Thr-85 O*H* hydrogen bond as the most probable situation to account for the above observation. The finding of a Thr-85

Table V: Dependence of NH Chemical Shifts ($\delta_{DMSO/CDCl_3} - \delta_{DMSO}$) on Solvent Composition in $CDCl_3$/DMSO Mixture (2/1) for Peptide III (The Peptides Are Insoluble in Pure Chloroform)

	residue								
	Leu-81	Arg-82	Tyr-83	Ser-84	Thr-85	Gly-86	Thr-87	Val-88	Cys-89
Δδ (ppm)	+0.09	−0.36	−0.04	−0.67	+0.08	+0.23	−0.54	−0.15	−0.5

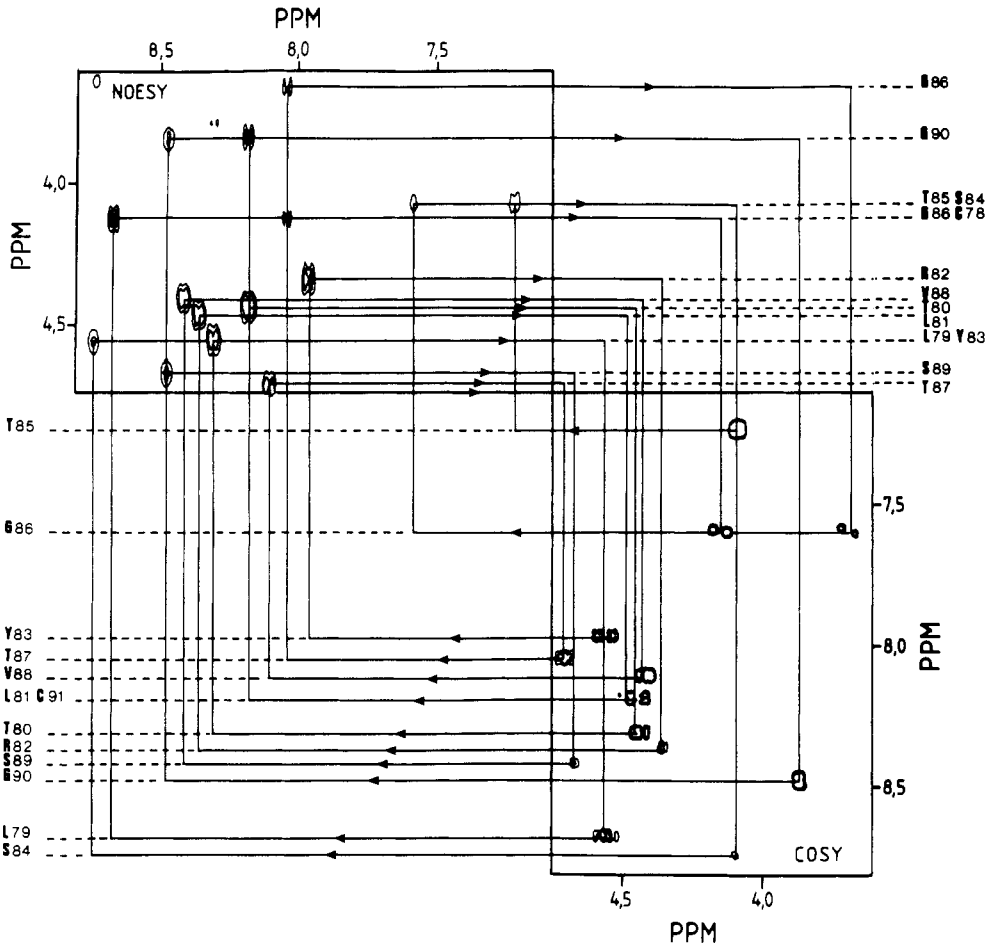

FIGURE 5: Combined COSY/NOESY connectivity for sequential resonance assignments via NOEs between NH and $C_\alpha H$ protons of the preceding residue. In the upper left the region 3.60–4.75 ppm × 8.80–7.10 ppm from the NOESY spectrum with mixing time 300 ms is presented. In the lower right is the corresponding COSY region. The arrows indicate the connectivities between neighboring residues.

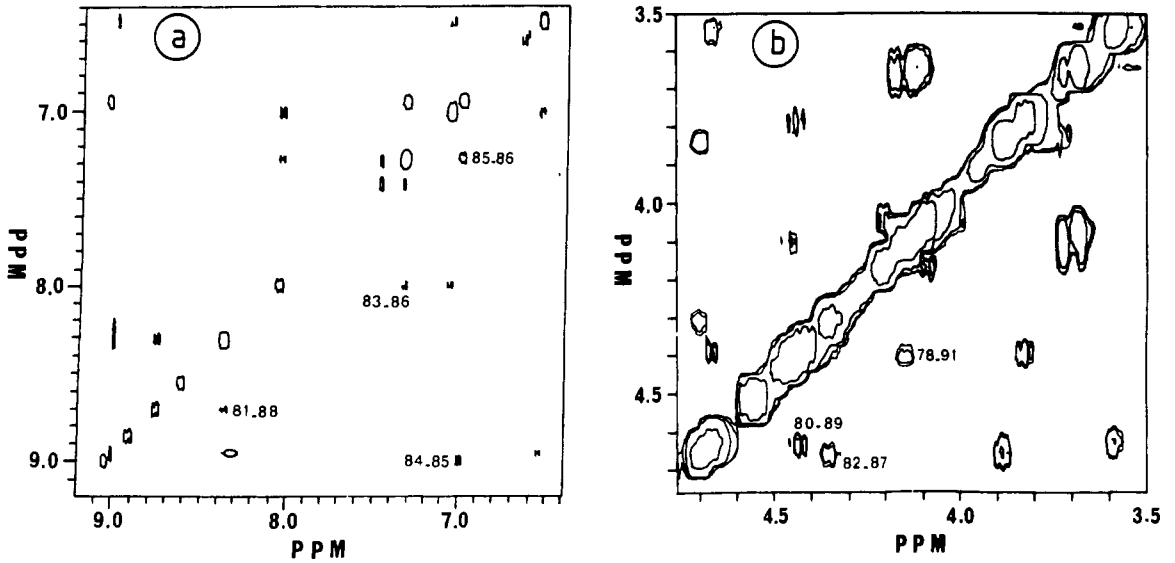

FIGURE 6: Spectral region from contour plot 360-MHz ^{1}H NOESY spectra of peptides III and IV: (a) spectral region (ω_1 = 6.4–9.2 ppm, ω_2 = 6.4–9.2 ppm) of peptide III; (b) spectral region (ω_1 = 3.6–4.75 ppm, ω_2 = 3.6–4.75 ppm) of peptide IV. The cross-peaks arising from the short distances N*H*–N*H* and $C_\alpha H$–$C_\alpha H$ are indicated with the corresponding amino acid sequence numbers.

βH–Gly-86 N*H* NOE is in full agreement with such a feature of the Thr-85 side chain.

The Model. All the data discussed above lead us to propose for peptides III and IV the models shown in Figure 8. As already mentioned, the antiparallel strands are characterized by an antiparallel disposition of successive NH bonds and therefore successive CO bonds. Thus, owing to chirality of the residues, all residues have of course the L chirality, and the side chains point alternatively up and down from the mean plane of the sheet. For example in peptide IV those of Cys-78, Thr-80, Arg-82, Thr-87, Ser-89, and Cys-91 point down while the others, except those of the residues forming the turn, point up. Thus, the disulfide bridge is located on the same side as the polar side chains.

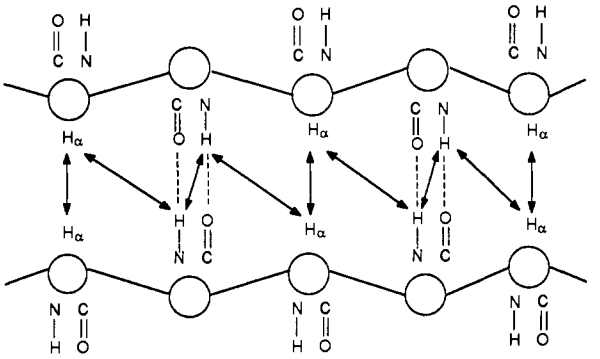

FIGURE 7: Schematic representation of a typical antiparallel β sheet. Dashed lines and arrows represent the characteristic hydrogen bonds and all the interstrands NOES, respectively.

This model holds true for peptide II at least in the turn region with a pronounced ability to induce the formation of the antiparallel β sheet structure as revealed by the finding of an Arg-82 $C_\alpha H$–Thr-87 $C_\alpha H$ NOE. A precise extension of this sheet structure could not be established due to the overlapping of the Thr-80 and Ser-89 $C_\alpha H$ resonances (see Table III). Concerning peptide I, as no interstrand NOEs could be detected, it is probably very flexible however with the presence of the β turn as suggested by the similarities between the temperature coefficients of peptides I and II especially for Ser-84 (see Table II).

Peptides Antigenicity: Recognition by Renin Antibodies

The ability of all four peptides to bind polyclonal human renin antibodies was tested by ELISA and the results are gathered in Table VI. It clearly appears that the linear peptides (I and II) were not recognized by any renin antibodies while the two cyclic compounds were. These results call for several comments. They suggest that both cyclic peptides adopt a conformation possibly similar or very near to that of the flap of human renin. Moreover the cyclic flap peptides are recognized by all the renin antibodies, indicating that the flap seems to overlap an important antigenic region of human renin. It is noteworthy that the nonlocked models (peptides I and II), which still contain the turn region in their structure, are not recognized by the antibodies. This may suggest that recognition by renin antibodies requires the presence of two antiparallel strands bearing probably some antigenic residues. This latter point questions the role of the turn. Is it necessary for immune recognition or does it only exist for the stability of the β structure? Work is now in progress to elucidate this point.

Table VI: Recognition of Peptides by Polyclonal Human Anti-Renin Antibodies[a]

renin antiserum	peptide I	peptide II	peptide III	peptide IV
R11	<2	<2	<2	<2
R12	<2	<2	4.7	5.8
R14	<2	<2	5.6	4.6
R15	<2	<2	7.9	5.3
R21	<2	<2	4.3	4.2
R22	<2	<2	6.8	5.6
R24	<2	<2	5.9	4.7
R25	<2	<2	7.0	9.2
R26	<2	<2	5.7	7.5
Donc	<2	<2	5.2	9.1
Bof	<2	<2	9.2	8.3

[a] The ELISA was performed as described under Materials and Methods. Results are expressed as A/A_0 ratio. Ratio < 2 is interpreted as nonsignificant binding.

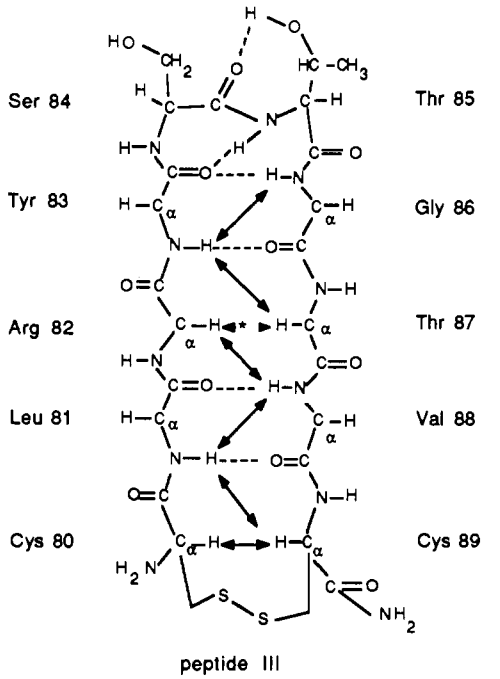

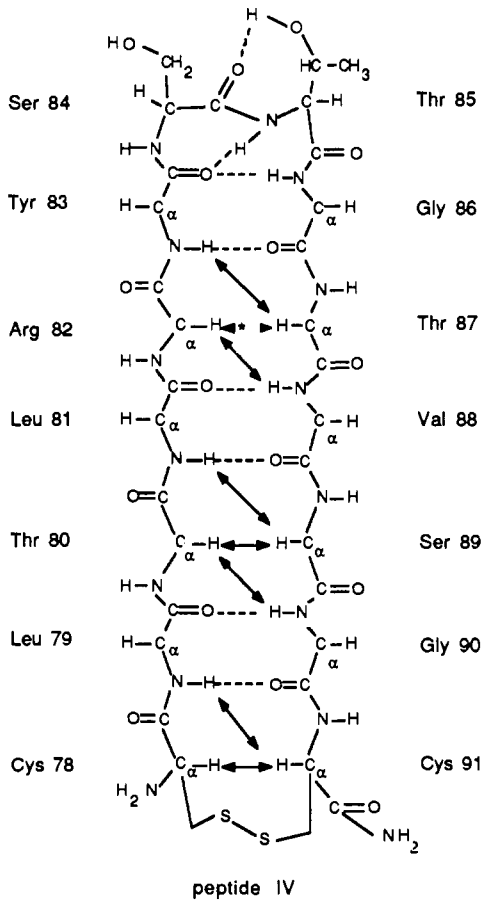

FIGURE 8: Schematic drawing of the proposed conformations for peptides III and IV. Dashed lines represent hydrogen bonds and arrows observed interstrands NOEs; asterisks (*) represent observed NOEs in peptide II.

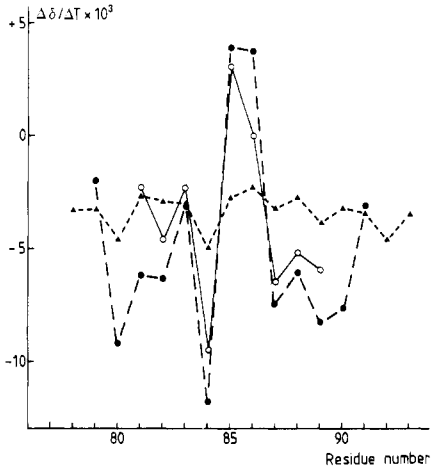

FIGURE 9: Variations along the peptides chains of the temperature coefficients ($\Delta\delta/\Delta T$) of the NH groups: (▲) II; (○) III; (●) IV. Coefficients of peptide I are not represented for clarity because they are very close to that of peptide II.

CONCLUSIONS

From the above investigations it can be concluded that the two cyclic peptides adopt in DMSO a secondary structure close to that expected in human renin while the linear ones are more flexible. The β hairpin loop structure is strongly stabilized by the presence of a disulfide bridge which acts in a similar manner as the remainder of the protein as revealed by the ability of cyclic peptides to bind human renin antisera. Therefore these peptides are good tools to verify the concept of using peptides, i.e., small segments of a protein, as haptens. These haptens may be used for the detection of predicted proteins from their gene sequences as well as for mapping of proteins in view of obtaining synthetic vaccines.

ACKNOWLEDGMENTS

We thank Dr. T. Blundell for the communication of his human and submaxillary renins models. Our thanks are due to Pr. L. Maury for giving access to the infrared spectrometer, A. Padilla for NMR program modifications, and A. Sahuquet and M. Passama for technical assistance.

Registry No. Peptide I, 105568-44-3; peptide II, 114096-11-6; peptide III, 114096-13-8; peptide III reduced, 114096-12-7; peptide IV, 114096-15-0; peptide IV reduced, 114096-14-9; renin, 9015-94-5.

REFERENCES

Akahane, K., Umeyama, H., Nakagawa, S., Moriguchi, I., Hirose, S., Iizuka, K., & Murakami, K. (1985) *Hypertension (Dallas) 7*, 3–12.

Aue, W. P., Bartholdi, E., & Ernst, R. R. (1976) *J. Chem. Phys. 64*, 2229–2246.

Billeter, M., Braun, W., & Wuthrich, K. (1982) *J. Mol. Biol. 15*, 321–346.

Blundell, T., Sibanda, B. L., & Pearl, L. (1983) *Nature (London) 304*, 273–275.

Bodenhausen, G., Kogler, H., & Ernst, R. R. (1984) *J. Magn. Reson. 58*, 370–388.

Carlson, W., Karplus, M., & Haber, E. (1985) *Hypertension 7*, 13–26.

Chou, P. Y., & Fasman, G. D. (1978) *Adv. Enzymol. Relat. Areas Mol. Biol. 47*, 45–148.

Dormoy, J. R., & Castro, B. (1979) *Tetrahedron Lett. 35* 3321–3322.

Evin, G., Carlson, W. D., Handschumacher, M., Novotny, J., Matsueda, G. R., Haber, E., Bouhnik, J., Galen, F. X., Menard, J., & Corvol, P. (1986) *Hypertension 8 (Suppl. II)*, II-72–II-77.

Galen, F. X., Devaux, C., Guyenne, T., Mênard, J., & Corvol, P. (1979) *J. Biol. Chem. 254*, 4848–4855.

Galen, F. X., Devaux, C., Atlas, S., Guyenne, T., Mênard, J., Corvol, P., Simon, D., Cazaubon, C., Richer, P., Badouaille, G., Richaud, J. P., Gros, P., & Pau, B. (1984) *J. Clin. Invest. 74*, 723–735.

Gierasch, L. M., Deber, C. M., Madison, V., Nice, C. H., & Blout, E. R. (1981) *Biochemistry 20*, 4730–4738.

Imai, T., Miyazuki, H., Hirose, S., Hori, H., Hayashi, T., Kageyama, R., Ohkubo, H., Nakanishi, S., & Murakami, K. (1983) *Proc. Natl. Acad. Sci. U.S.A. 80*, 7405–7409.

James, M. N. G., & Sielecki, A. R. (1985) *Biochemistry 24*, 3701–3713.

James, M. N. G., & Sielecki, A. R. (1986) *Nature (London) 319*, 33–38.

Kishore, R., & Balaram, P. (1984) *J. Chem. Soc., Chem. Commun.*, 778–781.

Kuo, M., & Gibbons, W. A. (1980) *Biophys. J. 32*, 807–836.

Le Nguyen, D., & Rivier, J. (1986) *Int. J. Pept. Protein Res. 27*, 285–292.

Nagayama, K., Kumar, A., Wuthrich, K., & Ernst, R. R. (1980) *J. Magn. Reson. 40*, 321–334.

Otting, G., Widmer, H., Wagner, G., & Wuthrich, K. (1986) *J. Magn. Reson. 66*, 187–193.

Pardi, A., Billeter, M., & Wuthrich, K. (1984) *J. Mol. Biol. 180*, 741–751.

Sibanda, B. L., Blundell, T., Hobart, P. M., Fogliano, M., Bindra, J. S., Dominy, B. W., & Chirgwin, J. M. (1984) *FEBS Lett. 174*, 102–111.

Tang, J., James, M. N. G., Hsu, I. N., Jenkins, J. A., & Blundell, T. L. (1978) *Nature (London) 271*, 618–621.

Wagner, G. (1983) *J. Magn. Reson. 55*, 151–156.

Wagner, G., Kumar, A., & Wuthrich, K. (1981) *Eur. J. Biochem. 114*, 375–384.

Wuthrich, K. (1983) *Biopolymers 22*, 131–138.

Wuthrich, K., Billeter, M., & Braun, W. (1984) *J. Mol. Biol. 180*, 715–740.